Electroacupuncture combined with rTMS promotes neuronal regeneration *via* DNMT1-mediated PI3K-AKT pathway in cerebral palsy model

Juan Fan,[1] Yu Ma,[1] Liying Sun,[1] Suhua Miao,[1] Jianghong He[2]

[1]Tsinghua University Yuquan Hospital, Beijing; [2]Tiantan Hospital, Capital Medical University, Beijing, China

ABSTRACT

Cerebral palsy (CP), resulting from perinatal brain injury, is characterized by persistent motor dysfunction largely due to impaired regeneration of the corticospinal tract. Electroacupuncture (EA) and repetitive transcranial magnetic stimulation (rTMS) are promising non-invasive neuromodulation approaches, but their combined effects and epigenetic mechanisms remain unclear. This study examined the synergistic neurorestorative potential of EA and rTMS in a hypoxic–ischemic brain damage (HIBD) model of CP, focusing on DNA methyltransferase 1 (DNMT1) regulation of the PI3K-AKT pathway. *In vivo*, neonatal rats subjected to HIBD were assigned to control, HIBD, EA, rTMS, or combined EA+rTMS groups and treated for four weeks. Motor function was assessed using rotarod, grid-walking, and grip strength tests, while neuronal and molecular changes were analyzed via histological and biochemical methods. *In vitro*, hypoxia-exposed cortical neurons underwent DNMT1 and PI3K modulation to clarify mechanisms. Combined EA+rTMS produced superior functional recovery compared to monotherapies, including a 2.1-fold increase in rotarod latency, 53% reduction in foot faults, and 80% improvement in grip strength vs untreated HIBD animals. Improvements were also greater than EA or rTMS alone. Histological findings showed enhanced neuronal density in cortical and spinal regions. At the molecular level, combined treatment suppressed DNMT1 expression and increased PI3K, phosphorylated AKT, GAP-43, and myelin basic protein. In vitro, DNMT1 knockdown enhanced PI3K-AKT signaling, neuronal survival, and axonal growth, while DNMT1 overexpression or PI3K inhibition negated these effects. Overall, EA+rTMS promotes functional and structural recovery in CP by epigenetically inhibiting DNMT1 and activating the PI3K-AKT pathway, supporting its translational potential for perinatal brain injury.

Key words: electroacupuncture; repetitive transcranial magnetic stimulation; cerebral palsy; neuronal regeneration; DNMT1; epigenetic regulation; PI3K-AKT pathway.

Correspondence: Jianghong He, MD, Tiantan Hospital, Capital Medical University, No. 5, Shijingshan Road, Shijingshan District, Beijing 100040, China. E-mail: 13581984292@163.com

Conflict of interest: the authors declare no competing interests.

Contributions: Juan Fan, Jianghong He, designed the study and performed the experiments; Yu Ma, Liying Sun, collected the data; Yu Ma, Liying Sun, Suhua Miao analyzed the data. Juan Fan, Jianghong He, prepared the manuscript. All authors read and approved the final manuscript and agreed to be accountable for all aspects of the work

Ethical approval and consent to participate: all procedures complied with NIH Guide for the Care and Use of Laboratory Animals and were approved by the Animal Ethics Committee of Tiantan Hospital Animal Center (23-CMU-51-004).

Funding: this work was supported by the Beijing Natural Science Foundation - Haidian Original Innovation Joint Fund Project (Project Number: L222154) “Research on Key Technologies of Minimally invasive Implantation Robot with Flexible Electrodes for the Mechanism of STN-DBS in the Treatment of Parkinson's Disease”.

Availability of data and materials: the data that support the findings of this study are available from the corresponding author upon reasonable request.

Introduction

Cerebral Palsy (CP) is a non-progressive disorder of the central nervous system (CNS) arising from early brain injury, primarily characterized by impairments in motor function and postural control.[1] Its core pathology involves damage to or maldevelopment of the corticospinal tract (CST), which critically connects the cerebral cortex to the spinal cord, resulting in severely restricted motor control capabilities.[2] While existing rehabilitative strategies, pharmacological interventions, and surgical procedures can ameliorate symptoms in some patients, their efficacy remains limited, particularly concerning the inadequate promotion of neural axonal regeneration.[1,2]

Recent advancements in neural regeneration and functional recovery within the CNS have centered on several therapeutic approaches. These include strategies to overcome the intrinsic inhibitory environment of the CNS and enhance axonal regrowth. One approach is the use of growth factors, such as neurotrophins, delivered via innovative drug delivery systems to promote tissue remodeling and neural regeneration.[3] Additionally, activation of transcription factors has shown promise in stimulating axon regeneration in the CNS, although achieving robust regeneration and meaningful functional recovery remains challenging.[4] Electrical stimulation techniques have also emerged as a promising tool, enhancing neural plasticity and supporting motor and sensory recovery by activating axon growth-associated genes.[5] Despite these developments, the limitations of current therapies, including the poor intrinsic regenerative capacity of adult CNS neurons and the persistent environmental inhibitors, continue to impede the full functional recovery of patients with CNS injuries. Consequently, developing effective strategies to facilitate CST regeneration and repair, thereby fundamentally improving motor function in CP patients, represents a major research priority and challenge.

Electroacupuncture (EA) and repetitive Transcranial Magnetic Stimulation (rTMS) are two non-invasive therapeutic modalities showing promise in promoting neural regeneration and functional recovery within the CNS. Research indicates that EA can enhance neuronal survival and axonal regrowth by modulating neurotransmitter release and neurotrophic factor expression.[6] Conversely, rTMS promotes motor recovery by regulating cortical excitability and enhancing neuroplasticity.[7] However, each modality has inherent limitations. EA's effects may be spatially constrained, primarily influencing neural circuits near stimulation sites or specific pathways, potentially limiting its impact on widespread CST damage.[8] rTMS effects, while modulating cortical excitability, can be transient and may not adequately address peripheral neuromuscular components or deep structural connectivity deficits crucial in CP.[9] Consequently, monotherapy with either approach may be insufficient for comprehensively improving the complex interplay of central and peripheral nervous system dysfunction in CP.

Combining these two neuromodulation modalities represents a targeted complementary strategy to mitigate these limitations, as it can simultaneously address the spatial constraints of EA and the transient, functionally restricted effects of rTMS. This establishes a clear rationale for investigating the synergistic effects of combined EA and rTMS, as well as their underlying regulatory mechanisms in CP.

DNA methylation, a key epigenetic regulatory mechanism, plays a pivotal role in nervous system development, function, and repair. DNA methyltransferase 1 (DNMT1) is a principal enzyme governing DNA methylation status, influencing critical cellular processes like proliferation, differentiation, and apoptosis through gene methylation.[10] Recent research highlights the significant role of the PI3K-AKT signaling pathway in neural regeneration and repair, promoting axonal growth and functional recovery by regulating neurotrophic factors and neuroprotective proteins.[11] Therefore, elucidating how DNMT1-mediated DNA methylation regulates the PI3K-AKT pathway is crucial for understanding its role in CP neurorepair and revealing novel therapeutic targets. Notably, emerging evidence suggests neuromodulation techniques can influence DNA methylation. EA has been shown to modulate methylation enzymes, for instance, triggering TREM2 DNA methylation to ameliorate Alzheimer's disease (AD) in model mice[12] and downregulating DNMT1 to alleviate anxiety in mice.[13] Similarly, rTMS has also been demonstrated to regulate DNA methylation patterns.[14]

However, research on the combined application of EA and rTMS for targeting methylation pathways is scarce. This study employs in vivo and in vitro experiments to investigate the regulatory effects of combined EA and rTMS on the DNMT1-mediated PI3K-AKT signaling pathway, aiming to delineate its specific mechanism of action in CP treatment and provide a theoretical foundation for optimizing clinical therapeutic strategies.

Materials and Methods

Animal study

A total of 120 male SD rat pups (postnatal day 7, P7, 12-15 g) were supplied by the Guangdong Laidi Biomedical Research Institute. Animals were housed in specific pathogen-free (SPF) conditions at the Tiantan Hospital Animal Experimental Center. The housing environment maintained a temperature of 22±2°C, 50-60% humidity, and a 12-h light/dark cycle with ad libitum access to food and water.

The hypoxic-ischemic brain damage (HIBD) model was induced in P7 SD rat pups as previously described with modifications.[15] Briefly, pups were anesthetized with pentobarbital sodium (Sigma-Aldrich, St. Louis, MO, USA; P3761; 40 mg/kg, i.p.). Under a stereomicroscope, the left common carotid artery was isolated, doubly ligated with 4-0 silk sutures, and transected. After a 120-min recovery period with the dam, pups were exposed to 8% O_2 in a hypoxic chamber at 37°C for 3 h. Sham controls underwent anesthesia and incision without ligation or hypoxia.

HIBD-modeled pups were randomly assigned to 5 groups (n=6/group): 1) Control: Sham surgery + no treatment; 2) Model: HIBD + no treatment; (3) EA: HIBD + electroacupuncture at Baihui (GV20) and bilateral Zusanli (ST36) (20-30 min/day, 2 Hz, 1 mA).[16] 3) rTMS: HIBD + high-frequency rTMS (15 Hz, 1.2 T, 10 min/day) over bilateral motor cortices[17]; 4) EA+rTMS: HIBD + combined EA and rTMS (EA followed by rTMS). The sample size (n=6/group) was determined based on pre-experimental data, which confirmed that 6 animals per group provided sufficient statistical power to detect significant intergroup differences in behavioral and molecular outcomes while ensuring experimental reproducibility. Treatments started 24 h post-modeling and continued for 4 weeks.

Behavioral assessments for motor function recovery[18] were performed at designated time points: baseline (2 days post-modeling, prior to any treatment initiation), midpoint (2 weeks after treatment initiation), and endpoint (24 h after the completion of the 4-week treatment regimen). All tests were conducted by experimenters blinded to the group allocation of the animals. The battery consisted of three validated tests for evaluating motor function recovery:

i) Rotarod test (motor coordination and balance): animals were acclimated to the stationary rod (XR-6C; Shanghai Xinruan, Shanghai, China) for 15 min on the day preceding testing. During the test phase, rat were placed on the rotating rod (rotating away from the animal) and subjected to an accelerating protocol from 4 rpm to 40 rpm over a 5-min period. The primary outcome measure was the latency to fall (seconds). Each mouse underwent 3 trials per testing session, with an inter-trial rest interval of at least 15 min. The maximum score was capped at 300 s.

2) Grid-walking test (gait analysis and fine motor function): rat were tested on an elevated stainless steel grid apparatus (grid dimensions 41 x 41 cm, grid spacing 3.5 x 3.5 cm, height 41 cm) after a 30-min habituation period to a large open field. For testing, the mouse was gently positioned in the center of the grid. Once the animal grasped the grid with all four paws, the grid was swiftly inverted 180 degrees, forcing the animal to walk while inverted for 60 s. The entire session was video-recorded. The primary outcome was the percentage of foot faults, calculated as the number of limb slips (where a paw completely missed the grid rung) divided by the total number of steps taken during the 60-s observation period, multiplied by 100. The grid surface was thoroughly cleaned with 70% ethanol before and after each animal to eliminate odor cues.

iii) Grip strength test (forelimb and hindlimb muscle force): limb strength was assessed using a grip strength meter (XR501; Shanghai Xinruan) equipped with a thin wire grid (max 2000 g capacity, 0.1g resolution). The meter was zeroed before each session. Animals were briefly acclimated to holding the grid. The assessor gently grasped the mouse by the base of the tail and lowered it horizontally towards the grid, allowing only the forepaws to grasp. The tail was then steadily pulled backward horizontally at approximately 10 cm/s until the animal released its grip. The peak grip force (grams) displayed was recorded. The procedure was repeated 3 times consecutively for the forelimbs, with a 1-2 minute rest between trials. The peak grip force for each animal was calculated as the average of three valid trials.

At the study endpoint (24 h post-treatment), rats were deeply anesthetized with i.p. pentobarbital sodium (PB, 50 mg/kg). Upon loss of pedal reflex, euthanasia was performed via cervical dislocation. The brain and spinal cord were rapidly dissected. Tissues for molecular analysis were snap-frozen in LN□ and stored at −80°C. Samples for histology/IF were fixed in 10% formalin for 24 h at RT before processing.

Cell culture

Primary rat cortical neurons were isolated from the cerebral cortices of 1- to 2-day-old male SD rats (Guangdong Laidi Biopharmaceutical Co., Ltd., Guangzhou, China) as previously described. Briefly, dissected cortices were digested at 37°C for 15 min in 0.25% trypsin (R001100; Gibco, Rockville, MD, USA) containing 0.02% EDTA. Digestion was terminated by adding Dulbecco's Modified Eagle Medium/Nutrient Mixture F-12 (DMEM/F12; 11320033; Gibco) supplemented with 10% fetal bovine serum (FBS; FSD500, Excell Bio, Suzhou, China). The digested tissue was filtered through a 100-μm cell strainer to obtain a single-cell suspension. Neurons were seeded onto poly-D-lysine-coated culture vessels (Jet BIOFIL) and maintained in Neurobasal-A medium (10888022; Gibco) supplemented with 1× B-27™ Plus supplement (A3582801; Gibco), 2 mM L-glutamine (A2916801; Gibco), and 1% penicillin-streptomycin solution (C0222; Beyotime, Shanghai, China). Cultures were incubated at 37°C in a humidified atmosphere with 5% CO_2.

Experimental groups and treatments applied to these neurons were as follows: 1) Control group: Neurons cultured under standard conditions without hypoxia or any treatment. 2) Hypoxia group: neurons exposed to humidified gas mixture (90% humidified N_2, 5% O_2, and 5% CO_2) for 3 h using a hypoxic chamber (Coy Laboratory Products);[19] this oxygen concentration was selected to recapitulate the pathological hypoxic microenvironment of perinatal hypoxic-ischemic brain injury underlying CP, and has been widely validated and adopted in established primary cortical neuron hypoxia models for preclinical CP research. 3) Hypoxia + DNMT1-KD group: following 3 h of hypoxia, neurons were transfected with DNMT1 siRNA (100 nM total concentration, custom sequence; Sangon Biotech, Shanghai, China) using Lipofectamine 3000 (L3000015; ThermoFisher, Waltham, MA, USA) and Opti-MEM (31985070; ThermoFisher) for 6 h, then cultured for an additional 24 h in Neurobasal-A medium under normoxia. 4) Hypoxia + DNMT1-OE group: following 3 h of hypoxia, neurons were transfected with the overexpression plasmid pcDNA3.1-DNMT1 (custom construction targeting NM_053354.3:81-4946; Sangon Biotech, Shanghai, China) using Lipofectamine 3000 and Opti-MEM for 6 h, then cultured for an additional 24 h in Neurobasal-A medium under normoxia. 5) Hypoxia + PI3K inhibition group: following 3 hof hypoxia, neurons were treated with the PI3K inhibitor LY294002 (HY-10108; MedChemExpress, Monmouth Junction, NJ, USA) at a final concentration of 20 μM in Neurobasal-A medium and incubated under normoxia for 24 h.[20] 6) Hypoxia + DNMT1-KD + PI3K-OE group: following 3 h of hypoxia, neurons were co-transfected with DNMT1 siRNA and the overexpression plasmid pcDNA3.1-PI3K (custom construction targeting NM_001371300.3:178-3486; Sangon Biotech) using Lipofectamine 3000 and Opti-MEM for 6 h, then cultured for an additional 24 h in Neurobasal-A medium under normoxia. Non-targeting siRNA (si-NC) and empty vector (pcDNA3.1) controls were used in relevant experiments.

Plasmid construction and transfection

Plasmid construction

The overexpression plasmids for rat DNMT1 (pcDNA3.1-DNMT1) and rat PI3K (pcDNA3.1-PI3K) were custom-constructed by Sangon Biotech. Both constructs utilized the pcDNA3.1(+) mammalian expression vector. The full-length coding sequence (CDS) of the rat Dnmt1 gene (NCBI Reference Sequence: NM_053354.3, bases 81-4946) and the rat Pik3ca gene (NCBI Reference Sequence: NM_001371300.3, bases 178-3486) were inserted into the vector's multiple cloning site. The sequences of the final constructs were verified by Sangon Biotech prior to use. The empty pcDNA3.1(+) vector was used as a negative control for overexpression experiments.

siRNA design

Three specific small interfering RNAs (siRNAs) targeting the rat Dnmt1 transcript were designed based on the sequence NM_053354.3 and synthesized by Sangon Biotech (Shanghai, China). The siRNA sequences, including the non-targeting control siRNA (si-NC), are listed in Table 1.

Primary rat cortical neurons were plated on PDL-coated 6-well plates and transfected at 80% confluency. For plasmid transfection (overexpressing DNMT1 or PI3K), Lip3000 reagent was diluted in Opti-MEM and combined with plasmid DNA (2.5 μg/well) and P3000 enhancer. After 15 min at RT, complexes were added dropwise to cells and incubated 6 h at 37°C/5% CO_2. The medium was then replaced with fresh Neurobasal-A containing B-27™ Plus, GlutaMAX, and antibiotics. Cells were cultured 24 h before harvesting. For siRNA knockdown (targeting DNMT1), a pool of three validated siRNAs (100 nM/well) was diluted in Opti-MEM, mixed with Lip3000, and incubated 15 min at RT. Complexes were

applied to cells for 6 h under standard conditions, after which the medium was replaced. Analysis was performed after 24 h.

Cell viability assay

Cell viability was assessed with a CCK-8 kit (BA00208; Bioss, Woburn, MA, USA). Primary cortical neurons were plated in 96-well plates at 5×10³ cells/well, pre-incubated for 6 h (37°C, 5% CO□), and treated per experimental design. After 24 h, 10 µL CCK-8 reagent was added to each well. Following 2 h of incubation in darkness, the absorbance at 450 nm was recorded using a microplate reader (Thermo Scientific). Results were normalized to the control group.

qPCR

Total RNA was extracted with an isolation kit (RC112; Vazyme, Nanjing, China). RNA quality was verified (A260/A280 >1.8) using a spectrophotometer (Jiapeng). cDNA was synthesized from 500 ng RNA using HiScript III cDNA Synthesis Kit (R312; Vazyme, Nanjing, China). qPCR was performed using SYBR Master Mix (Q712; Vazyme) on a CFX96 system (Bio-Rad, Hercules, CA, USA). Cycling conditions: 95°C for 30 s; 40 cycles of 95°C/10 s and 60°C/10 s; melt curve analysis. All primers are listed in Table 2. Relative gene expression was calculated using the 2−ΔΔCt method.

Western blot

Proteins were extracted using RIPA buffer with PMSF. Concentration was determined by BCA assay. Samples (30 µg/lane) were separated *via* 12% SDS-PAGE and transferred to PVDF membranes. After blocking with 5% non-fat milk, membranes were incubated with primary antibodies at 4°C overnight: GAP-43 (ab75810; Abcam, Cambridge, MA, USA), MBP (ab7349, Abcam), PI3K (#4292; Cell Signaling Technology, Inc., Danvers, MA, USA), AKT (#9272; Cell Signaling Technology, Inc.), mTOR (C#2972; Cell Signaling Technology, Inc.), p-AKT (#9271; Cell Signaling Technology, Inc.), DNMT1 (#5032; Cell Signaling Technology, Inc.), GAPDH (ab8245; Abcam). HRP-conjugated secondary antibodies (bs-0295G/0296G; Bioss) were applied for 2 h at RT. Signals were developed with ECL and quantified using ImageJ.

Immunofluorescence

Spinal cord and cortical sections (3.5 µm) were treated with 0.1% poly-L-lysine (P-8920; Sigma-Aldrich) for 10 min and air-dried. After fixation in 10% formalin (24 h), tissues were dehydrated through an ethanol gradient (70-100%, 40 min each), paraffin-embedded, and sectioned onto PLL-coated slides. Slides were baked (50°C, 60 min), deparaffinized with Histoclear II, rehydrated in ethanol series and ddH□O, and subjected to microwave-based antigen retrieval in appropriate buffer.

The sections were blocked with blocking buffer for 1 h, and then incubated overnight at 4°C in a humidified, dark chamber with primary antibodies (1:1000 dilution): GAP-43 (ab75810; Abcam), DNMT1 (#5032; Cell Signaling Technology, Inc.), and PI3K (#4292; Cell Signaling Technology, Inc.). After incubation, the slides were washed three times with PBS. Next, secondary antibodies (1:2000 dilution), either Goat Anti-Rabbit IgG H&L/HRP (bs-0295G-HRP; Bioss) or Goat Anti-Mouse IgG H&L/HRP (bs-0296G-HRP; Bioss), were applied and incubated at room temperature for 1 h in a dark, humidified chamber. Finally, the sections were stained with DAPI (C1006; Beyotime) for 5 min, washed three times with PBS, and observed under a fluorescence microscope.

Cell immunofluorescence staining

Primary cortical neurons were processed according to their respective groups. The cells were first gently washed three times with PBS and then fixed with 1 mL of 4% paraformaldehyde for 20 min. After fixation, the cells were permeabilized with 0.25% Triton X-100 for 20 min and blocked with 1 mL of goat serum for 30 min. Following blocking, the cells were incubated overnight at 4°C with primary antibodies (1:500-1000 dilution): DNMT1 (#5032; Cell Signaling Technology, Inc.), GAP-43 (ab75810; Abcam), and SAP102 (ab316858; Abcam). The next day, the cells

Table 1. siRNA sequences targeting rat Dnmt1 (NM_053354.3).

siRNA designation	Sequence (5'→3')
DNMT1 siRNA-1	Sense: 5'-UGGUAGAAGUAGGUCUUCCCA-3' Antisense: 3'-GGAAGACCUACUUCUACCAGU-5'
DNMT1 siRNA-2	Sense: 5'-ACUUGUGGGUGUUCUCAGGCC-3' Antisense: 3'-CCUGAGAACACCCACAAGUCC-5'
DNMT1 siRNA-3	Sense: 5'-ACACAUCCAGGGUCCGCAGCU-3' Antisense: 3'-CUGCGGACCCUGGAUGUGUUU-5'
si-NC	Sense: 5'-UUCUCCGAACGUGUCACGUTT-3' Antisense: 5'-ACGUGACACGUUCGGAGAATT-3'

Table 2. siRNA sequences targeting rat Dnmt1 (NM_053354.3).

Gene	Forward primer (5'→3')	Reverse primer (5'→3')
DNMT1	CGGTTATTCGGCAACATCCTGCTTTAACTGCAGCTGAGGCACT	
GAP-43	AGGGAGATGGCTCTGCTACTGACGGCGAGTTATCAGTGGT	
MBP	GCATCCTTGACTCCATCGGGTACGCCTCGGAGCTCACCT	
PI3K	ACACGGGGGCATTCAAAGATGTCGTTGTGCCTGTCACCTA	
AKT	CCTGGACTACTTGCACTCCGCACAGCCCGAAGTCCGTTAT	
GAPDH	TCTCTGCTCCTCCCTGTTCTTACGGCCAAATCCGTTCACA	

were washed three times with PBS and then incubated with secondary antibodies (1:1000 dilution) at room temperature for 1 h in the dark. After staining with DAPI, the cells were washed with PBS and mounted with Fluoroshield®. Fluorescence was observed under a fluorescence microscope, and fluorescence intensity was quantified using ImageJ software.

Nissl staining of rat brain tissue

Rat brain tissues were fixed in 10% formalin (24 h), dehydrated in graded ethanol, cleared in xylene, and embedded in paraffin. Sections (5 μm) were mounted, dried at 37°C, deparaffinized, and rehydrated. Staining was performed using Nissl stain (C0117; Beyotime) for 5 min. After dehydration and clearing, sections were mounted with neutral gum and imaged under a light microscope (Zeiss, Oberkochen, Germany).

Data analysis and statistics

Normality was assessed using Shapiro-Wilk test. For two-group comparisons, Student's *t*-test or Mann-Whitney U test was applied. Multiple groups were analyzed by one-way ANOVA (Tukey's *post-hoc*) or Kruskal–Wallis test (Dunn's correction). Data are presented as mean ± SD from ≥3 replicates. Significance was set at *p<0.05, **p<0.01, ***p<0.001. GraphPad Prism (Version X; La Jolla, CA, USA) and ImageJ were used for analysis and visualization.

Results

Electroacupuncture combined with rTMS improves motor function recovery and upregulates neuroprotective protein expression in cerebral palsy rats

Behavioral assessments revealed that EA combined with rTMS significantly improved motor function recovery in the HIBD-induced cerebral palsy rat model. In the longest residence time, grid walking, and grip power tests, the EA + rTMS group demonstrated notable improvements in motor function recovery, especially at the endpoint of the 4-week treatment regimen, with significant increases observed in all three tests compared to the model group (p<0.001). Although both EA and rTMS individually also showed some improvement in motor function recovery, the combination of both treatments yielded the most substantial recovery. Western blot analysis showed that the EA + rTMS treatment significantly upregulated the expression of GAP-43, MBP, PI3K, AKT, p-AKT, while significantly downregulated the expression of DNMT1, indicating enhanced axonal regeneration and activation of the PI3K-AKT signaling pathway. Specifically, GAP-43 and MBP, key markers for neuronal regeneration, were significantly elevated in the EA + rTMS group compared to the model group, with statistically significant differences (p<0.01, p<0.001). qRT-PCR results further confirmed the upregulation of GAP-43, MBP,

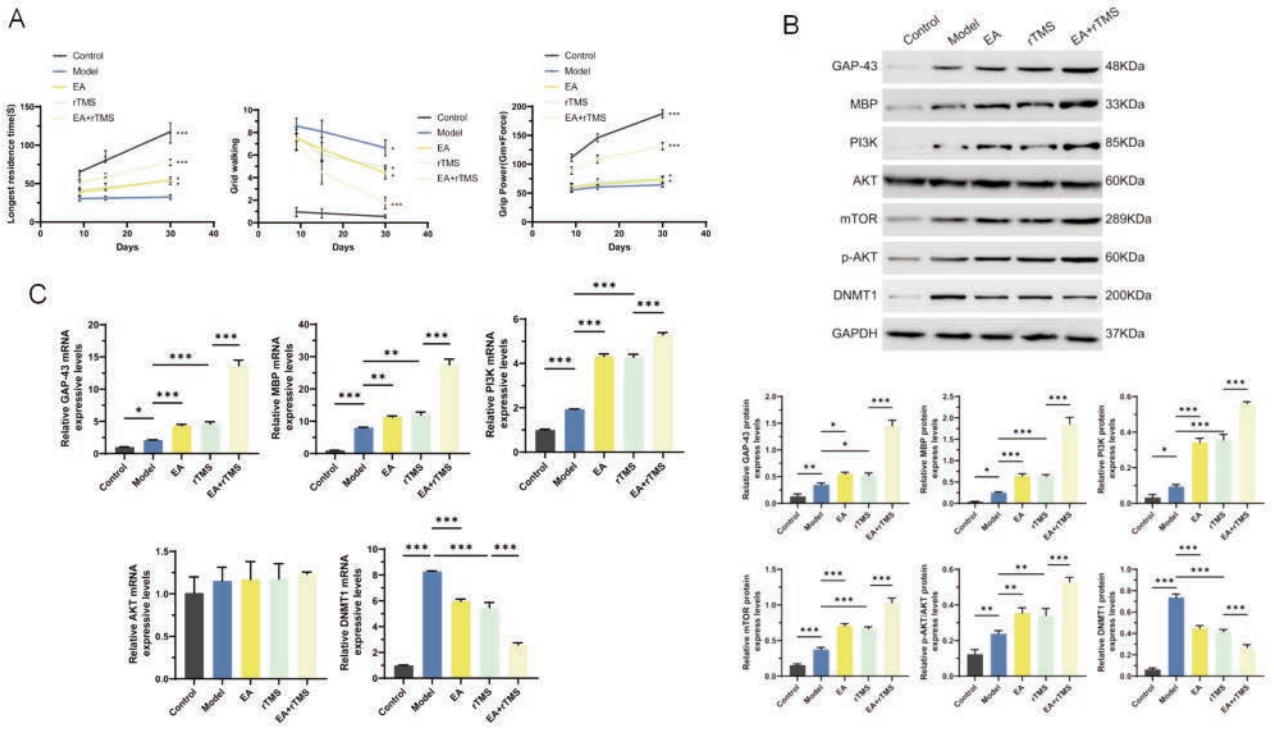

Figure 1. Effects of electroacupuncture (EA) combined with repetitive transcranial magnetic stimulation (rTMS) on motor function and neuroregeneration-related protein expression in the HIBD-induced cerebral palsy rat model. **A**) Behavioral assessments of rotarod latency, grid-walking test, and grip strength test across the Control, HIBD Model, EA, rTMS, and EA+rTMS groups. **B**) Western blot analysis of protein expression levels for GAP-43, MBP, PI3K, total AKT, phosphorylated AKT (p-AKT), and DNMT1. **C**) Quantitative real-time PCR (qRT-PCR) analysis of mRNA expression levels for GAP-43, MBP, PI3K, total AKT, and DNMT1. Data are presented as mean ± SD (n=6 rats per group); *p<0.05, ***p<0.01, ****p<0.001.

and PI3K gene expression in the EA + rTMS group, with statistically significant differences observed compared to the model group (p<0.01). Overall, these findings suggest that EA combined with rTMS promotes motor function recovery and axonal regeneration through the activation of the PI3K-AKT pathway (Figure 1).

Electroacupuncture combined with rTMS enhances neuronal regeneration in the spinal cord and cortex

Nissl staining (Figure 2A) showed that the Control group had intact neuronal morphology with abundant Nissl bodies, while the Model group exhibited a reduction in neuronal density. Both the EA and rTMS groups showed some improvement in neuronal density and morphology, but the EA + rTMS group demonstrated the greatest improvement in both aspects, with significantly higher neuronal counts. Immunofluorescence staining of the spinal cord (Figure 2B) revealed that the Model group exhibited elevated expression of GAP-43, DNMT1, and PI3K. The EA and rTMS groups both showed increased expression of GAP-43 and PI3K compared to the Model group, although DNMT1 expression was reduced (p<0.001). The EA + rTMS group displayed the highest levels of GAP-43 and PI3K, suggesting enhanced axonal regeneration, while DNMT1 expression remained the lowest (p<0.001). Similar findings were observed in the cortex (Figure 2C), where the EA + rTMS group had the highest expression of GAP-43 and PI3K, and the lowest DNMT1 expression (p 0.001). These results collectively suggest that electroacupuncture combined with rTMS promotes neuronal regeneration in both the spinal cord and cortex by enhancing the expression of regeneration-related proteins such as GAP-43 and PI3K, while reducing inhibitory factors like DNMT1.

DNMT1 knockdown enhances PI3K-AKT signaling and promotes axonal regeneration in hypoxia-exposed cortical neurons

To further investigate the role of DNMT1-mediated DNA methylation in regulating the PI3K-AKT pathway during axonal regeneration, we examined protein and mRNA expression in primary rat cortical neurons under various conditions. Western blot analysis (Figure 3A) revealed that hypoxia significantly increased DNMT1, PI3K, p-AKT, and GAP-43 protein expression compared to the control group (p<0.001). DNMT1 knockdown in hypoxic neurons decreased DNMT1 expression (p<0.001) while enhancing PI3K (p<0.001), p-AKT (p<0.01), and GAP-43 (p<0.01) levels compared to hypoxia alone. Conversely, DNMT1 overexpression increased DNMT1 protein (p<0.001) while reducing PI3K (p<0.001), p-AKT (p<0.01), and GAP-43 (p<0.001) levels. PI3K inhibition significantly decreased PI3K (p<0.001), p-AKT (p<0.001), and GAP-43 (p<0.001) expression, and also reduced DNMT1 levels (p<0.01). Combined DNMT1 knockdown with PI3K overexpression produced the lowest DNMT1 expression and highest PI3K, p-AKT, and GAP-43 protein levels (all p<0.001 compared to DNMT1 knockdown alone). Parallel qRT-PCR analysis (Figure 3B) demonstrated similar patterns in mRNA expression for DNMT1, PI3K, and GAP-43 across all groups, while AKT mRNA levels remained unchanged, suggesting post-transcriptional regulation. These findings indicate that DNMT1-mediated DNA methylation negatively regulates the PI3K-AKT pathway and subsequent axonal regeneration in cortical neurons under hypoxic conditions.

DNMT1 knockdown enhances cell viability and axonal growth through PI3K-AKT pathway activation in hypoxic conditions

Cell viability assays demonstrated that hypoxia significantly increased cell viability compared to control conditions (p<0.01) (Figure 4A). DNMT1 knockdown further enhanced cell viability under hypoxic conditions (p<0.001 compared to hypoxia alone), while both DNMT1 overexpression and PI3K inhibition significantly reduced cell viability (p<0.001 compared to hypoxia alone). The combination of DNMT1 knockdown with PI3K overexpression produced the highest cell viability among all treatment groups (p<0.001 compared to both hypoxia alone and DNMT1 knockdown alone), showing a significant increase compared to control.

Immunofluorescence analysis revealed that hypoxia significantly increased both DNMT1 (p<0.001) and GAP-43 (p<0.01) expression compared to control conditions (Figure 4B). DNMT1 knockdown under hypoxic conditions significantly decreased DNMT1 expression (p<0.001) while further enhancing GAP-43 levels (p<0.001). Conversely, DNMT1 overexpression increased DNMT1 fluorescence intensity (p<0.001) while reducing GAP-43 expression (p<0.001). PI3K inhibition decreased both DNMT1 (p<0.001) and GAP-43 expression (p<0.001). The combination of DNMT1 knockdown with PI3K overexpression produced the lowest DNMT1 expression (p<0.001 compared to hypoxia alone) and highest GAP-43 levels (p<0.001 compared to hypoxia alone), with a significant increase in GAP-43 compared to DNMT1 knockdown alone (p<0.001).

Axonal growth assessment showed that hypoxia significantly increased axonal length compared to control conditions (p<0.001) (Figure 4C). DNMT1 knockdown further enhanced axonal growth under hypoxic conditions (p<0.001), while both DNMT1 overexpression and PI3K inhibition significantly reduced axonal length (p<0.001 and p<0.01, respectively, compared to hypoxia alone). The combination of DNMT1 knockdown with PI3K overexpression resulted in the greatest axonal growth among all treatment groups (p<0.001 compared to hypoxia alone), with axons approximately twice as long as those in the control group and significantly longer than in the DNMT1 knockdown group (p<0.001). These findings collectively suggest that DNMT1 knockdown promotes neuronal survival and axonal regeneration through enhanced activation of the PI3K-AKT pathway under hypoxic conditions, with a clear dose-dependent relationship observed across all measured parameters.

Discussion

This study demonstrates that the combined application of EA at GV20 and ST36 acupoints with high-frequency rTMS significantly improves motor function and promotes neuronal regeneration in a neonatal HIBD model, serving as a cerebral palsy surrogate. The synergistic effect surpasses either intervention alone, highlighting a novel non-invasive combinatorial therapeutic approach. Crucially, our findings reveal that this functional recovery is mechanistically linked to the downregulation of DNMT1, which subsequently alleviates its inhibitory effect on the PI3K-AKT signaling pathway, culminating in enhanced expression of neuroregenerative markers like GAP-43 and MBP.

The robust improvement in rotarod performance, grid-walking accuracy, and grip strength observed in the EA+rTMS group underscores the therapeutic potential of simultaneously targeting peripheral neuromodulation (*via* EA) and cortical excitability (*via* rTMS). This aligns with emerging evidence suggesting combinatorial neuromodulation strategies yield superior outcomes in neurorehabilitation by engaging complementary repair mechanisms.[21] EA is known to enhance neurotrophic factor release and regional blood flow,[22] while high-frequency rTMS promotes cortical plas-

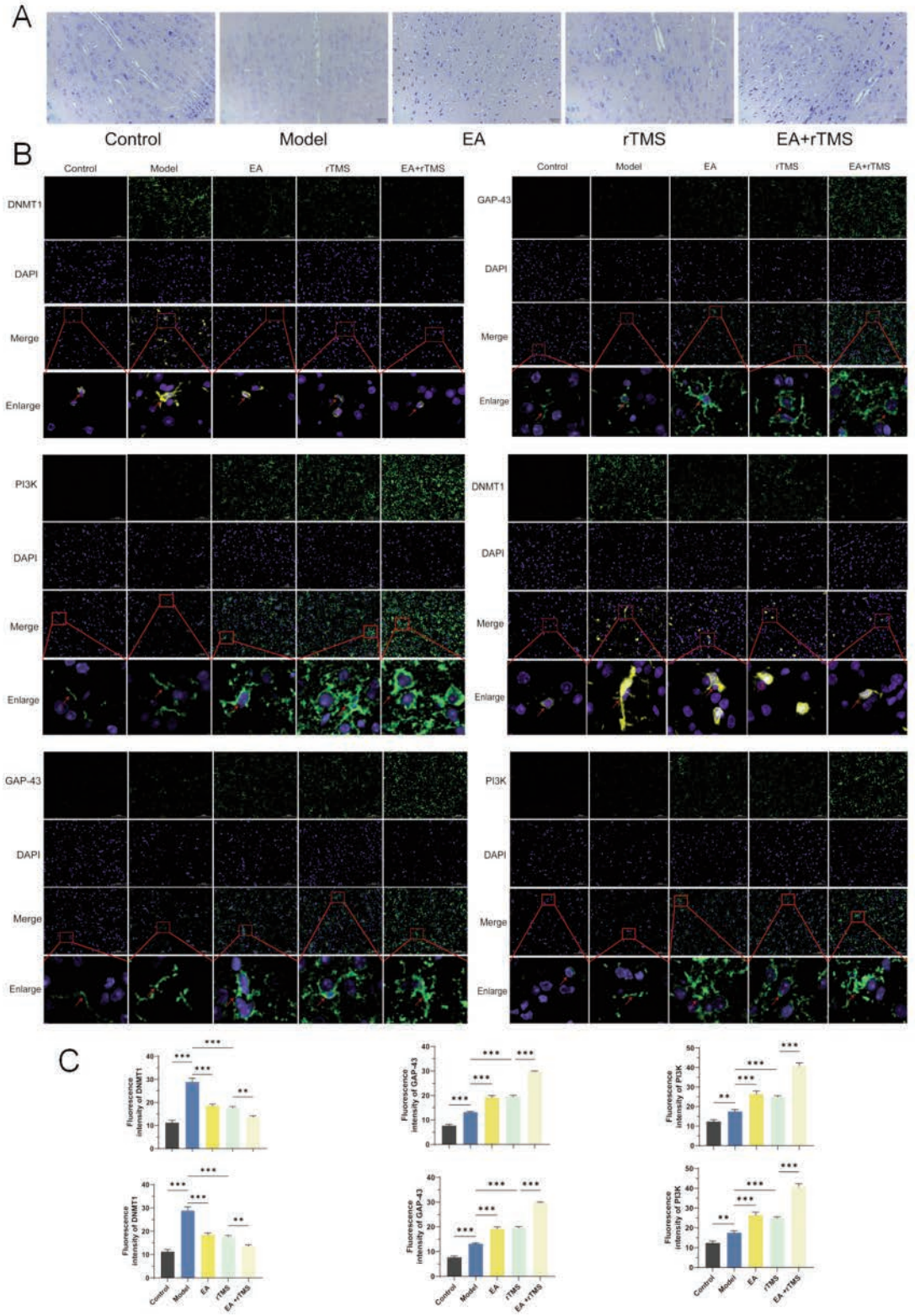

Figure 2. Electroacupuncture (EA) combined with repetitive transcranial magnetic stimulation (rTMS) enhances neuronal regeneration and modulates DNMT1, GAP-43, and PI3K expression in the rat spinal cord and cerebral cortex. **A**) Nissl staining showing neuronal morphology and density in the cerebral cortex across the Control, HIBD Model, EA, rTMS, and EA+rTMS groups, with the EA+rTMS group demonstrating the greatest improvement in neuronal integrity; magnification: 200×. **B**) Immunofluorescence staining of DNMT1, GAP-43, and PI3K (with DAPI nuclear counterstain) in the spinal cord and cerebral cortex across all experimental groups; magnification: 200×. **C**) Quantitative analysis of relative fluorescence intensity for DNMT1, GAP-43, and PI3K from the immunofluorescence staining assays. Data are presented as mean ±SD (n=6 rats per group); *p<0.05, **p<0.01, ***p<0.001.

ticity and neurogenesis.[23] Our data extend this understanding, demonstrating that their sequential application (EA followed by rTMS) creates a permissive microenvironment for neural repair, significantly improving motor coordination, gait, and muscle strength more effectively than monotherapies. This synergistic effect likely arises from EA priming neural circuits, potentially enhancing cortical responsiveness to subsequent rTMS.[24] The timing of intervention initiation (24 h post-injury) and sustained duration (4 weeks) likely contributed to the observed efficacy, aligning with critical windows for neuroplasticity after perinatal brain injury.[25]

A central mechanistic insight from our *in vivo* data is the consistent downregulation of DNMT1 protein and mRNA in the EA+rTMS group within both spinal cord and cortical tissues, concomitant with the upregulation of PI3K, p-AKT, GAP-43, and MBP. This inverse relationship positions DNMT1, a key enzyme mediating DNA methylation, as a potential negative regulator of post-injury neural repair. This finding is substantiated by our in vitro experiments, where hypoxia itself induced DNMT1 upregulation. Crucially, DNMT1 knockdown under hypoxic conditions dramatically amplified PI3K-AKT pathway activation (increased PI3K and p-AKT), boosted the expression of the axonal growth marker GAP-43, enhanced neuronal viability, and significantly promoted axonal elongation. Conversely, DNMT1 overexpression or PI3K inhibition (using LY294002) reversed these beneficial effects. The most potent in vitro outcome was achieved by co-manipulating DNMT1 knockdown with PI3K overexpression, yielding the highest cell viability and axonal growth alongside minimal DNMT1 expression. This compellingly demonstrates a causal relationship where DNMT1 acts as a molecular brake on the pro-regenerative PI3K-AKT axis in neurons subjected to hypoxic stress. Mechanistically, we speculate that DNMT1 may directly suppress the PI3K-AKT signaling cascade by mediating hypermethylation of CpG islands in the promoter regions of core genes within this pathway, thereby transcriptionally silencing their expression and inhibiting downstream pro-regenerative signaling. Our results resonate with recent studies implicating DNMT1 in maintaining repressive epigenetic landscapes that hinder the expression of regeneration-associated genes (RAGs) after neural injury.[26] Hypoxia can induce widespread hypermethylation, silencing pro-survival and growth-promoting pathways.[27] The EA+rTMS combination appears to mitigate this epigenetic barrier, facilitating PI3K-AKT activation.

The PI3K-AKT pathway emerges as a critical convergence point mediating the neurorestorative effects observed both in vivo and in vitro. Its activation, evidenced by increased PI3K expression and AKT phosphorylation (p-AKT) in the EA+rTMS group and in DNMT1-knockdown neurons, orchestrates multiple facets of neural repair. AKT phosphorylation activates downstream effectors like mTOR, crucial for protein synthesis, neuronal growth, and survival.[28] The significant upregulation of GAP-43, a key protein involved in axonal sprouting and growth cone dynamics,[29] and

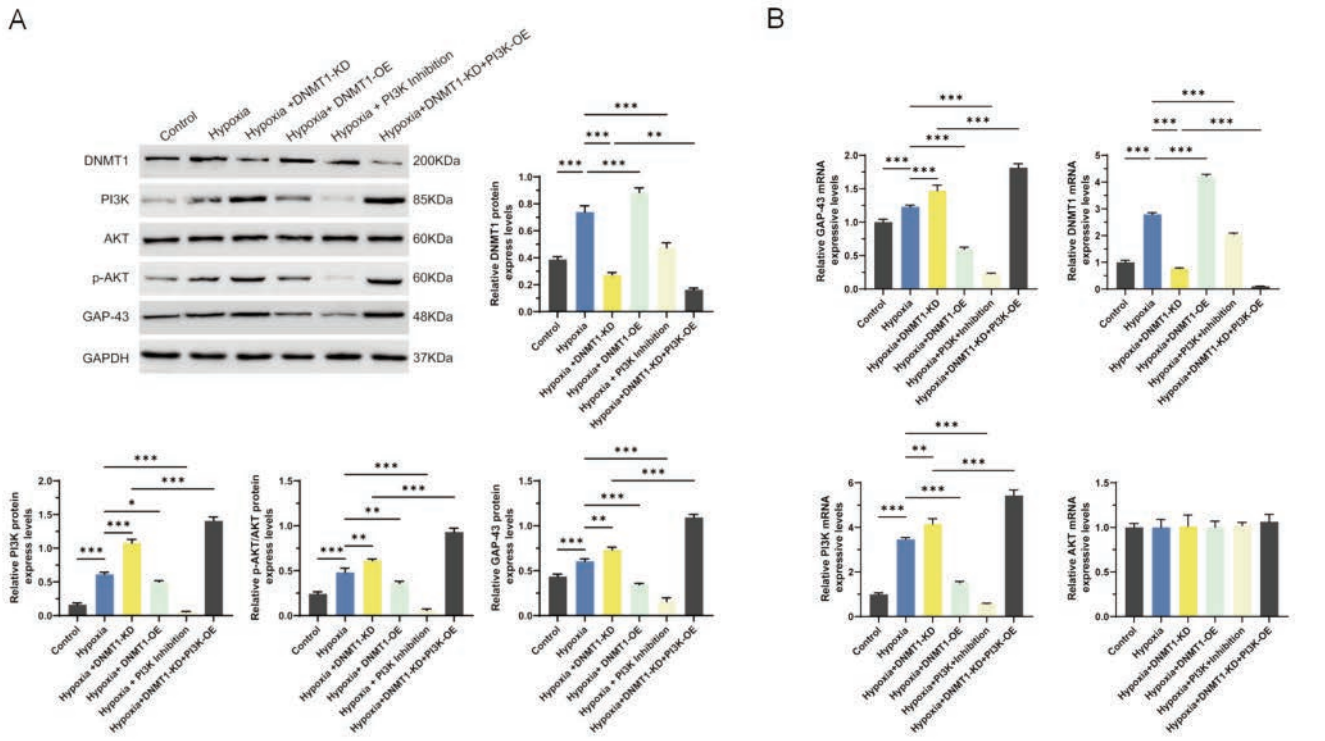

Figure 3. DNMT1 knockdown enhances PI3K-AKT signaling and promotes axonal regeneration in hypoxia-exposed primary rat cortical neurons. **A**) Western blot analysis of protein expression levels for DNMT1, PI3K, total AKT, phosphorylated AKT (p-AKT), and GAP-43 across the Control, Hypoxia, Hypoxia+DNMT1-KD, Hypoxia+DNMT1-OE, Hypoxia+PI3K Inhibition, and Hypoxia+DNMT1-KD+PI3K-OE groups, with corresponding quantitative analyses below. **B**) Quantitative real-time PCR (qRT-PCR) analysis of mRNA expression levels for DNMT1, PI3K, GAP-43, and total AKT in each experimental group. Data are presented as mean ±SD (n=6 independent replicates per group); *p<0.05, **p<0.01, ***p<0.001.

MBP, essential for myelination and conduction velocity,[30] downstream of PI3K-AKT activation, directly links this pathway to the structural and functional recovery observed. The fact that AKT mRNA levels remained unchanged across in vitro groups while p-AKT protein levels fluctuated significantly underscores the importance of post-transcriptional regulation and pathway activity (phosphorylation status) over mere gene expression in determining the regenerative outcome. This highlights PI3K-AKT signaling modulation, particularly through epigenetic regulation of DNMT1, as a promising therapeutic target.

The observed increase in neuronal viability and axonal growth in cortical neurons under hypoxia alone compared to normoxic controls is noteworthy. This potentially reflects an endogenous neuroprotective or preconditioning response to sublethal hypoxia, a phenomenon documented in some models.[31-33] However, our data clearly show that this intrinsic adaptive capacity can be substantially amplified by targeting the DNMT1-PI3K axis. DNMT1 knockdown or PI3K overexpression pushed viability and axonal growth far beyond the levels achieved by hypoxia alone. This suggests that while hypoxia may initiate some pro-survival signals, the

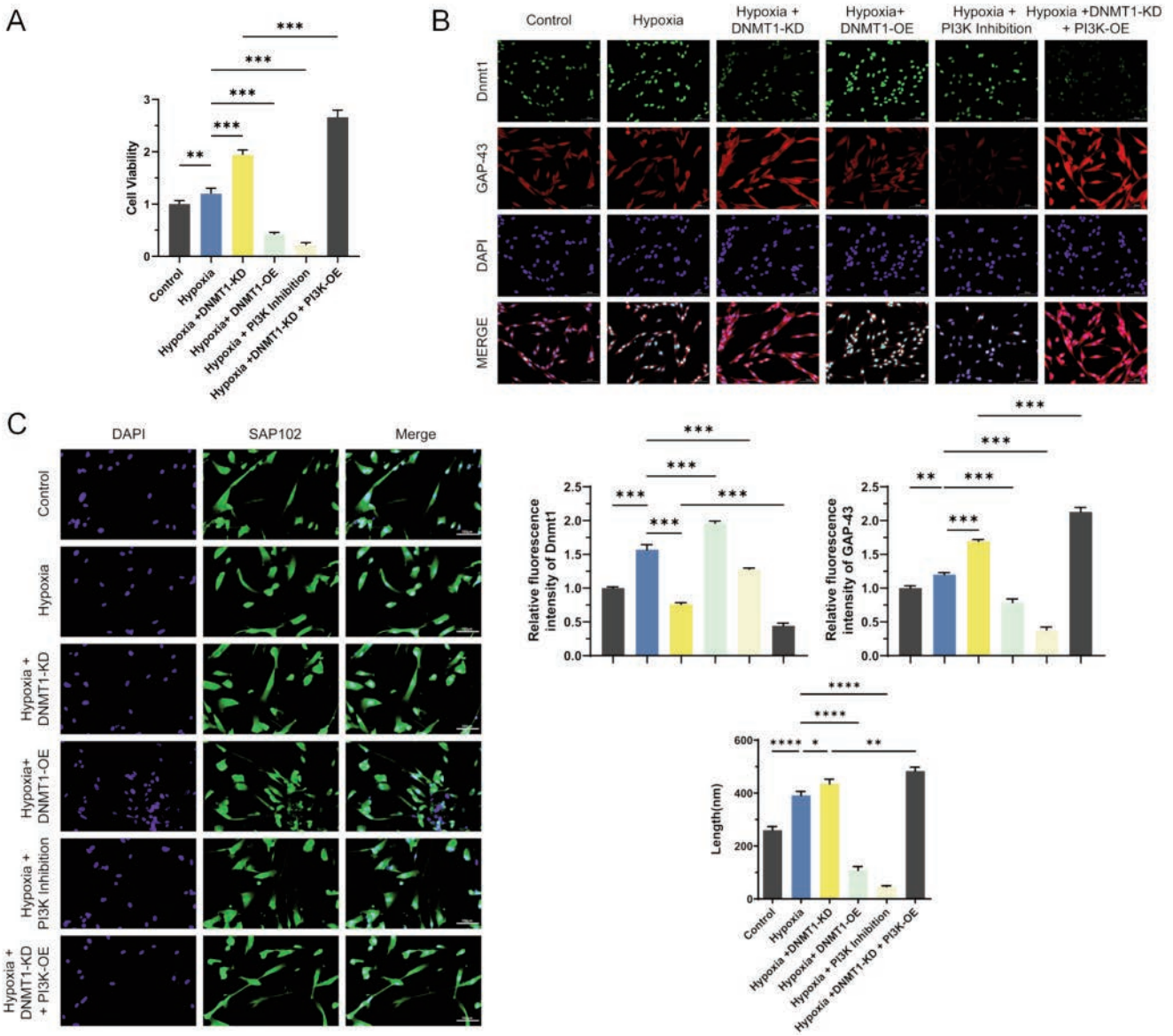

Figure 4. DNMT1 knockdown promotes cell viability and axonal regeneration in hypoxia-exposed primary rat cortical neurons. **A**) Cell viability detected by CCK-8 assay across the Control, Hypoxia, Hypoxia+DNMT1-KD, Hypoxia+DNMT1-OE, Hypoxia+PI3K Inhibition, and Hypoxia+DNMT1-KD+PI3K-OE groups. **B**) Immunofluorescence staining showing the distribution and expression of DNMT1 (green) and GAP-43 (red), with DAPI (blue) nuclear counterstain and merged images; quantitative analysis of relative fluorescence intensity for DNMT1 and GAP-43 is shown below; magnification: 200×. **C**) Axonal length assessment via SAP102 staining (green) with DAPI (blue) nuclear counterstain, and corresponding quantitative analysis of axonal length; magnification: 200×. Data are presented as mean ±SD (n=6 independent replicates per group); *p<0.05, **p<0.01, ***p<0.001.

concurrent upregulation of DNMT1 acts as a limiting factor. Therapeutic strategies like EA+rTMS, or direct molecular interventions targeting DNMT1, effectively remove this constraint, unlocking the full regenerative potential potentiated by the hypoxic stimulus.

The translational significance of these findings lies in addressing the profound unmet need for effective neurorestorative therapies in cerebral palsy. Current management primarily focuses on symptom mitigation and compensation.[34,35] Our study provides preclinical evidence supporting EA+rTMS as a strategy capable of modifying disease progression by promoting endogenous repair mechanisms. The non-invasive nature of both interventions enhances their potential suitability for the pediatric population, although rigorous safety and efficacy trials in children are imperative.[36] The identification of the DNMT1-PI3K-AKT axis offers novel molecular targets (e.g., DNMT1 inhibitors) for future drug development alongside neuromodulation approaches. Furthermore, monitoring DNMT1 levels or PI3K-AKT activity could potentially serve as biomarkers for treatment response.

Several limitations warrant consideration. Firstly, while we demonstrate a clear association between DNMT1 downregulation, PI3K-AKT activation, and improved outcomes, the precise genomic targets of DNMT1 methylation responsible for suppressing PI3K-AKT signaling in this context remain unidentified. Future studies employing techniques like methylated DNA immunoprecipitation sequencing (MeDIP-seq) or reduced representation bisulfite sequencing (RRBS) are needed to map the specific methylation changes induced by EA+rTMS or DNMT1 manipulation. Secondly, the HIBD model, while widely used, does not fully recapitulate the complex etiology and chronicity of human cerebral palsy. Investigations in more complex models or different injury paradigms would strengthen the generalizability of the findings. Thirdly, the study focused on relatively short-term outcomes (4 weeks post-treatment initiation). Longer-term studies are essential to determine the durability of the observed benefits and potential late effects. Fourthly, the experimental design involved simultaneous initiation of EA and rTMS. Exploring optimal sequencing, timing, and dosage parameters for the combinatorial therapy could further refine efficacy. Fifthly, the contribution of non-neuronal cells (e.g., astrocytes, microglia) influenced by EA+rTMS or DNMT1 modulation to the observed neuroprotection and regeneration was not assessed and merits investigation. We speculate that EA+rTMS may indirectly facilitate neuronal regeneration and functional recovery by modulating reactive astrocyte activation, inhibiting pro-inflammatory microglial polarization, and thereby mitigating the neuroinflammatory microenvironment that impedes neural repair after hypoxic-ischemic injury. Future research should also explore the interaction of this pathway with other critical regulators of neural repair, such as the PTEN/PI3K axis or other epigenetic modifiers. Finally, translating these promising preclinical results requires carefully designed clinical trials in children with cerebral palsy, prioritizing safety assessment and establishing optimal stimulation parameters for this vulnerable population. Investigating the potential of DNMT1 inhibitors, either alone or as adjuvants to neuromodulation, represents another exciting future direction.

In conclusion, this study provides compelling evidence that combining electroacupuncture with rTMS significantly enhances motor recovery and neuronal regeneration in a cerebral palsy model, outperforming either therapy alone. The underlying mechanism involves the downregulation of DNMT1, which relieves its suppression on the PI3K-AKT signaling pathway, leading to increased expression of key neuroregenerative proteins like GAP-43 and MBP. These findings establish the DNMT1-PI3K-AKT axis as a critical regulator of post-injury neural repair and highlight EA+rTMS as a promising, non-invasive combinatorial strategy, whose non-invasive profile avoids the inherent risks associated with invasive therapeutic interventions and renders it particularly suitable for the pediatric cerebral palsy population, worthy of further clinical exploration for cerebral palsy and potentially other perinatal brain injuries.

References

1. Colver A, Fairhurst C, Pharoah POD. Cerebral palsy. Lancet 2014;383:1240-9.
2. Pin TW, Elmasry J, Lewis J. Efficacy of botulinum toxin A in children with cerebral palsy in gross motor function classification system levels IV and V: a systematic review. Dev Med Child Neurol 2013;55:304-13.
3. Xu D, Wu D, Qin M, Nih LR, Liu C, Cao Z, et al. Efficient delivery of nerve growth factors to the central nervous system for neural regeneration. Adv Mater 2019;31:e1900727.
4. Jara JS, Agger S, Hollis ERN. Functional electrical stimulation and the modulation of the axon regeneration program. Front Cell Dev Biol 2020;8:736.
5. Stern S, Hilton BJ, Burnside ER, Dupraz S, Handley EE, Gonyer JM, et al. RhoA drives actin compaction to restrict axon regeneration and astrocyte reactivity after CNS injury. Neuron 2021;109:3436-55.
6. Li K, Wang X, Jiang Y, Zhang X, Liu Z, Yin T, et al. Early intervention attenuates synaptic plasticity impairment and neuroinflammation in 5xFAD mice. J Psychiatr Res 2021;136:204-16.
7. Liu J, Zhao W, Guo J, Kang K, Li H, Yang X, et al. Electroacupuncture alleviates motor dysfunction by regulating neuromuscular junction disruption and neuronal degeneration in SOD1(G93A) mice. Brain Res Bull 2024;216:111036.
8. Zhang Q, Zhou M, Huo M, Si Y, Zhang Y, Fang Y, et al. Mechanisms of acupuncture-electroacupuncture on inflammatory pain. Mol Pain 2023;19:17448069231202882.
9. Gillick B, Rich T, Nemanich S, Chen C, Menk J, Mueller B, et al. Transcranial direct current stimulation and constraint-induced therapy in cerebral palsy: A randomized, blinded, sham-controlled clinical trial. Eur J Paediatr Neuro 2018;22:358-68.
10. Yan L, Geng Q, Cao Z, Liu B, Li L, Lu P, et al. Insights into DNMT1 and programmed cell death in diseases. Biomed Pharmacother 2023;168:115753.
11. He X, Li Y, Deng B, Lin A, Zhang G, Ma M, et al. The PI3K/AKT signalling pathway in inflammation, cell death and glial scar formation after traumatic spinal cord injury: Mechanisms and therapeutic opportunities. Cell Proliferat 2022;55:e13275.
12. Jiang J, Liu H, Wang Z, Tian H, Wang S, Yang J, et al. Effects of electroacupuncture on DNA methylation of the TREM2 gene in senescence-accelerated mouse prone 8 mice. Acupunct Med 2022;40:463-9.
13. Li Y, Liu X, Fu Q, Fan W, Shao X, Fang J, et al. Electroacupuncture ameliorates depression-like behaviors comorbid to chronic neuropathic pain via Tet1-mediated restoration of adult neurogenesis. Stem Cells 2023;41:384-99.
14. Meneses-San Juan D, Lamas M, Ramírez-Rodríguez GB. Repetitive transcranial magnetic stimulation reduces depressive-like behaviors, modifies dendritic plasticity, and generates global epigenetic changes in the frontal cortex and hippocam-

pus in a rodent model of chronic stress. Cells 2023;12:2062.
15. Yao D, Zhang W, He X, Wang J, Jiang K, Zhao Z. Establishment and identification of a hypoxia-ischemia brain damage model in neonatal rats. Biomed Rep 2016;4:437-43.
16. Yang Y, Wu S, Ma S, Guan M, Wang J, Ren B. [Effect of electroacupuncture at "Baihui" (GV20) and "Zusanli" (ST36) on angiogenesis in the brain of middle cerebral artery occlusion rats based on HIF/VEGF/Notch signaling pathway].[Article in Chinese]. Zhen Ci Yan Jiu 2024;49:1030-9.
17. Loo CK, Sachdev PS, Haindl W, Wen W, Mitchell PB, Croker VM, et al. High (15 Hz) and low (1 Hz) frequency transcranial magnetic stimulation have different acute effects on regional cerebral blood flow in depressed patients. Psychol Med 2003;33:997-1006.
18. Corder KM, Hoffman JM, Sogorovic A, Austad SN. Behavioral comparison of the C57BL/6 inbred mouse strain and their CB6F1 siblings. Behav Process 2023;207:104836.
19. Tao W, Zhang X, Ding J, Yu S, Ge P, Han J, et al. The effect of propofol on hypoxia- and TNF-α-mediated BDNF/TrkB pathway dysregulation in primary rat hippocampal neurons. Cns Neurosci Ther 2022;28:761-74.
20. Lin L, Chen H, Zhang Y, Lin W, Liu Y, Li T, et al. IL-10 Protects neurites in oxygen-glucose-deprived cortical neurons through the PI3K/Akt pathway. Plos One 2015;10:e0136959.
21. Bolognini N, Russo C, Edwards DJ. The sensory side of post-stroke motor rehabilitation. Restor Neurol Neuros 2016;34:571-86.
22. Liu S, Wang Z, Su Y, Qi L, Yang W, Fu M, et al. A neuroanatomical basis for electroacupuncture to drive the vagal-adrenal axis. Nature 2021;598:641-5.
23. Dionisio A, Duarte IC, Patricio M, Castelo-Branco M. The use of repetitive transcranial magnetic stimulation for stroke rehabilitation: a systematic review. J Stroke Cerebrovasc 2018;27:1-31.
24. Li Z, Lin W, Qi R. [Kaiqiao Jieyin acupuncture combined with repetitive transcranial magnetic stimulation for post-stroke aphasia: a randomized controlled trial].[Article in Chinese]. Zhongguo Zhen Jiu 2023;43:25-8.
25. Felling RJ, Song H. Epigenetic mechanisms of neuroplasticity and the implications for stroke recovery. Exp Neurol 2015;268:37-45.
26. Hutson TH, Kathe C, Palmisano I, Bartholdi K, Hervera A, De Virgiliis F, et al. Cbp-dependent histone acetylation mediates axon regeneration induced by environmental enrichment in rodent spinal cord injury models. Sci Transl Med 2019;11
27. Hahn MA, Qiu R, Wu X, Li AX, Zhang H, Wang J, et al. Dynamics of 5-hydroxymethylcytosine and chromatin marks in mammalian neurogenesis. Cell Rep 2013;3:291-300.
28. Li S, Overman JJ, Katsman D, Kozlov SV, Donnelly CJ, Twiss JL, et al. An age-related sprouting transcriptome provides molecular control of axonal sprouting after stroke. Nat Neurosci 2010;13:1496-504.
29. Chung D, Shum A, Caraveo G. GAP-43 and BASP1 in Axon Regeneration: Implications for the Treatment of Neurodegenerative Diseases. Front Cell Dev Biol 2020;8: 567537.
30. Cammarota M, Boscia F. Contribution of oligodendrocytes, microglia, and astrocytes to myelin debris uptake in an explant model of inflammatory demyelination in rats. Cells 2023;2203.
31. Stetler RA, Leak RK, Gan Y, Li P, Zhang F, Hu X, et al. Preconditioning provides neuroprotection in models of CNS disease: paradigms and clinical significance. Prog Neurobiol 2014;114:58-83.
32. Choi H, Choi N, Park H, Lee K, Lee YJ, Koh S. Sublethal doses of zinc protect rat neural stem cells against hypoxia through activation of the PI3K pathway. Stem Cells Dev 2019;28:769-80.
33. Liu J, Gu Y, Guo M, Ji X. Neuroprotective effects and mechanisms of ischemic/hypoxic preconditioning on neurological diseases. Cns Neurosci Ther 2021;27:869-82.
34. Novak I, Morgan C, Fahey M, Finch-Edmondson M, Galea C, Hines A, et al. State of the evidence traffic lights 2019: systematic review of interventions for preventing and treating children with cerebral palsy. Curr Neurol Neurosci 2020;20:3.
35. Jackman M, Sakzewski L, Morgan C, Boyd RN, Brennan SE, Langdon K, et al. Interventions to improve physical function for children and young people with cerebral palsy: international clinical practice guideline. Dev Med Child Neurol 2022;64:536-49.
36. Arumi-Trujillo C, Verdejo-Amengual FJ, Martinez-Navarro O, Vink JJT, Valenzuela-Pascual F. The effectiveness of non-invasive brain stimulation in enhancing lower extremity function in children with spastic cerebral palsy: protocol for a systematic review and meta-analysis. MethodsX 2025;14:103141.

Received: 22 January 2026. Accepted: 11 March 2026.

Licensee PAGEPress, Italy
European Journal of Histochemistry 2026; 70:4533
doi:10.4081/ejh.2026.4533